BIOCHEMISTRY
including biophysical chemistry & molecular biology

Current Topic

pubs.acs.org/biochemistry

Photochemical Tools for Studying Metal Ion Signaling and Homeostasis

Hannah W. Mbatia[‡] and Shawn C. Burdette*[,†]

[†]Worcester Polytechnic Institute, 100 Institute Road, Worcester, Massachusetts 01609-2280, United States

[‡]University of Connecticut, 55 North Eagleville Road, Storrs, Connecticut 06269-3060, United States

ABSTRACT: Metal ions have well-established catalytic and structural roles in proteins. Much of the knowledge acquired about metalloenzymes has been derived using spectroscopic techniques and X-ray crystallography, but these methodologies are less effective for studying metal ions that are not tightly bound to biomacromolecules. In order to prevent deleterious chemistry, cells tightly regulate the uptake, distribution, and intracellular concentrations of metal ions. Investigation into these homeostasis mechanisms has necessitated the development of alternative ways to study metal ions. Photochemical tools such as small molecule and protein-based fluorescent sensors as well as photocaged complexes have provided insight into the homeostasis and signaling mechanisms of Ca^{2+}, Zn^{2+}, and Cu^{+}, but a comprehensive picture of metal ions in biology will require additional development of these techniques, which are reviewed in this Current Topics article.

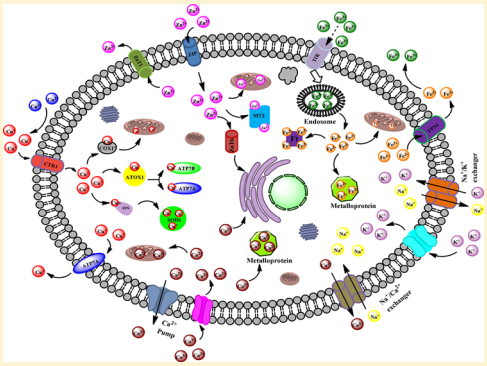

For decades, research in bioinorganic chemistry focused largely on metalloproteins and the few metal-based pharmaceuticals like cisplatin. The need to understand the coordination sphere and catalytic activity of Fe, Cu, Ni, and Co sites embedded in proteins helped drive the development of numerous techniques like electron paramagnetic resonance (EPR), Mössbauer and Raman spectroscopy. While these instrumental methods continue to be improved and expanded, their use has greatly facilitated and accelerated research on metal ions in biology.

The study of metal ion uptake and homeostasis occurred concurrently with other areas of inquiry in bioinorganic chemistry. With the exception of a few quintessential areas like iron,[1,2] metal ion homeostasis by proteins became a focal point recently. Current efforts have revealed the complex mechanisms that biology has evolved to handle metal ions. Permeases, uniporters, symports, antiporters, and chaperones act in concert to maintain cellular homeostasis (Figure 1).

Studying metal ion homeostasis often requires a different experimental approach than those developed for metalloproteins. Early work in the field of homeostasis has focused on the spectroscopically silent metal ions Ca^{2+} and Zn^{2+}, which eliminates the possibility of using many traditional instrumental techniques. In addition, detecting the slight homeostasis perturbations of a tightly regulated metal ion like Cu^{+}, which may be associated with disease states,[3] requires sensitive techniques. Over the past three decades, several approaches have been developed to probe metal ion homeostasis and signaling including small molecule sensors, protein-based sensors, and photocaged complexes.

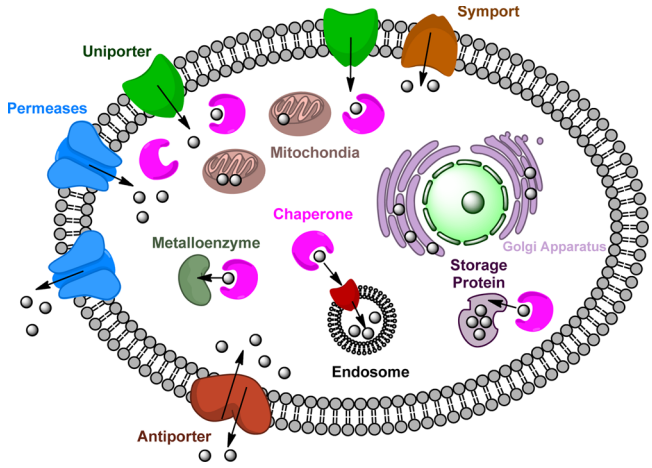

Figure 1. Simplified picture of metal ion homeostasis in cells. Emerging research indicates that cells maintain healthy levels of essential metal ions using several classes of proteins including permeases, uniporters, symporters, antiporters, and chaperones. Most of these proteins have evolved to traffic a specific metal ion by exploiting its unique inorganic chemistry.

SMALL MOLECULE SENSORS

The first widely used fluorescent sensors for metal ions were developed to monitor $[Ca^{2+}]$ associated with signal transduction.[4] Using the Ca^{2+} prototype, sensors for other

Received: February 7, 2012
Revised: August 13, 2012
Published: August 16, 2012

dx.doi.org/10.1021/bi3001769 | *Biochemistry* 2012, 51, 7212−7224

biologically important metal ions have been developed. An ideal sensor should selectively bind the analyte of interest with a dissociation constant near the median local concentration; in addition, receptor binding kinetics should allow for real-time monitoring of concentration fluctuations. The fluorophore should be photostable, absorb and emit with visible light, and exhibit significant changes in optical properties upon metal ion binding. After three decades of research, fluorescent sensor design has progressed from a trial and error approach to an established canon.[5] While challenges in sensor development remain, such as overcoming the inherent emission quenching of transition metal ions, the field can focus increasingly on studying unresolved issues in metal ion signaling and homeostasis.

Ca^{2+} Sensors. Calcium is involved in numerous processes including neurotransmission, muscle contraction, gene expression, and cell death. Parathyroid hormone in conjunction with Ca^{2+} pumps and channels regulate Ca^{2+} homeostasis.[6,7] Impaired regulation of intracellular Ca^{2+} ($[Ca^{2+}]_i$) can cause disease. Low levels of $[Ca^{2+}]_i$ contribute to heart failure while high $[Ca^{2+}]_i$ leads to cell death.[8] Fluorescent Ca^{2+} probes have been reviewed extensively,[4] so discussion will focus on recent advances.

Fluo-4 (log K = 6.5, K_d = 345 nM)[9] and the ratiometric probes Fura-2 (log K = 6.8, K_d = 145 nM) and Indo-1 (log K = 6.6, K_d = 230 nM)[10] have been used extensively to study Ca^{2+} signaling in many different cells (Figure 2). Ratiometric probes, where the apo- and metal-bound sensor absorb and/or emit at different wavelengths, allow for internal calibration of sensor concentration and distribution. These sensors utilize the high affinity Ca^{2+} chelator 1,2-bis(*o*-aminophenoxy)ethane-*N*,*N*,*N*′,*N*′-tetraacetic acid (BAPTA). In addition to satisfactory selectivity and fluorescence properties, these probes are commercially available so they have become the sensors of choice. Compartmentalization and the inability to target specific cell organelles limit the application of these probes; however, these sensors, and structural congeners, can be modified to address specific issues of Ca^{2+} homeostasis and signaling.

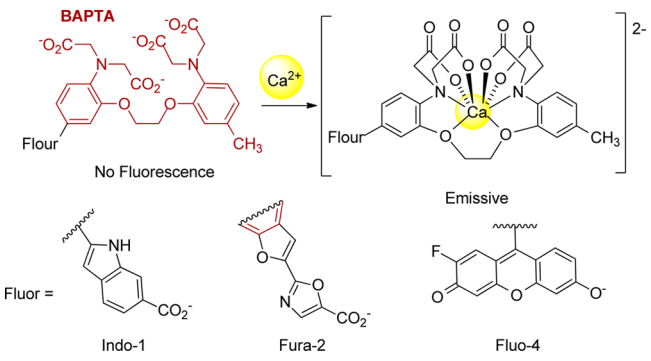

Figure 2. Structure of common fluorescent sensors for Ca^{2+}. In Indo-1 the fluorophore and BAPTA are conjugated via an aryl group, whereas in Fura-2 an aryl group from the BAPTA chelator is also part of the benzofuran fluorophore. Both constructs provide a ratiometric probe. Indo-1 exhibits ratiometric emission, whereas Fura-2 has ratiometric excitation. Fluo-4 has an electronically isolated BAPTA receptor and fluorophore, which provides an off-on fluorescence response.

Dextran-sensor conjugates modified with a localization peptide have been used to monitor Ca^{2+} dynamics in the nucleus;[11] however, membrane permeability issues require invasive techniques for cell introduction. Polystyrene microspheres enter cells passively and target the cytosol, which limits sequesterization issues. The Indo-1-microsphere probe exhibits enhanced cell permeability and does not require ester hydrolysis like the acetoxymethyl Ca^{2+} probes.[12] The sensor-microsphere dyad binds Ca^{2+} with log K = 6.6 (K_d = 226 nM) and a λ_{max} emission shift from 470 nm (apo) to 400 nm (complex). Since the attachment of the small molecule to the microsphere does not change the Ca^{2+}-binding or fluorescence properties significantly, adopting this strategy with other existing sensors would provide tools capable of monitoring a wider range of $[Ca^{2+}]_i$, which exemplifies the opportunities for advancing the understanding of Ca^{2+} biochemistry through probe development.

SNAP-tag technology provides an alternative to microspheres for controlling sensor localization. SNAP-tag, a mutant of the DNA repair protein O^6-alkylguanine-DNA alkyltransferase, reacts with a BG (O^6-benzylguanine) functionalized fluorophore to covalently label specific cellular compartments (Figure 3).[13,14] BOCA-1-BG incorporates the BG moiety with a BODIPY-based (boron-dipyrromethene) Ca^{2+} sensor.[15] The corresponding BOCA-1-SNAP Ca^{2+} probe exhibits a 180-fold fluorescence increase upon Ca^{2+} binding with log K = 6.7 (K_d = 200 nM). BOCA-1-SNAP can detect Ca^{2+} changes in the nuclei but with limited emission enhancement (<5-fold). When utilizing a ratiometric component, SNAP-3-Indo-1 exhibits a log K = 6.6 (K_d = 228 nM), and a λ_{max} emission shift from 469 nm (apo) to 420 nm (complex) in vitro, which are nearly identical to the parent sensor.[16,17] SNAP-3-Indo-1 shows that $[Ca^{2+}]$ in an isolated resting muscle cells of mice is approximately 50 nM. Like microspheres, SNAP-tag methods are readily adaptable and further probe development could rapidly advance the fields of Ca^{2+} homeostasis and signaling.

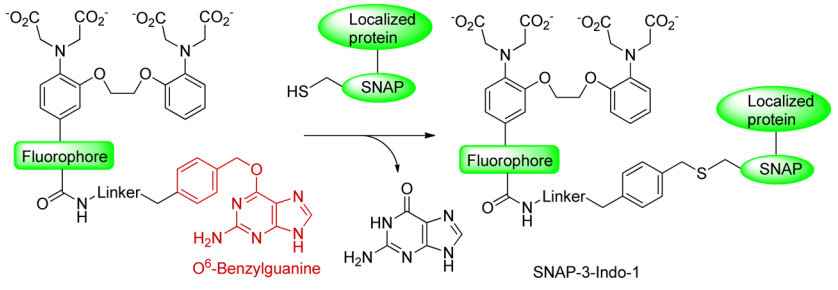

Figure 3. General construct in SNAP-tag Ca^{2+} sensing systems. A small molecule sensor linked to a BG group (red) can be attached to a protein containing the SNAP-tag.

dx.doi.org/10.1021/bi3001769 | *Biochemistry* 2012, 51, 7212−7224

Many Ca^{2+} sensors require near-UV excitation light that can cause cellular photodamage. Excitation at visible wavelengths is less harmful, but can still stimulate autofluorescence from endogenous fluorophores, which interferes with measurements. Near-infrared excitation overcomes these problems and can generate images of events occurring several hundred micrometers deep in tissues. KFCA utilizes the Keio Fluor-5 fluorophore and a BAPTA receptor (Figure 4).[18,19] KFCA

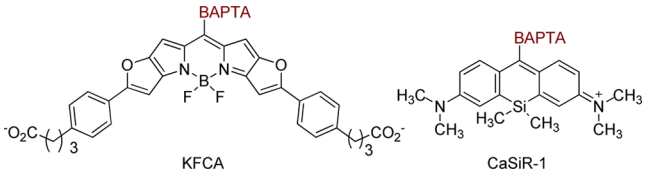

Figure 4. Structures of near-IR Ca^{2+} sensors KFCA and CaSiR-1. Both probes utilize the BAPTA (Figure 2) receptor utilized by traditional Ca^{2+} sensors.

binds Ca^{2+} with log K = 6.3 (K_d = 500 nM) and exhibits a 120-fold fluorescence enhancement at 670 nm. Employing HeLa cells, KFCA detects cytoplasmic Ca^{2+} changes following ATP stimulation. Similarly, CaSiR-1 incorporates a Si-rhodamine fluorophore with BAPTA.[20] CaSiR-1 binds Ca^{2+} with log K = 6.2 (K_d = 580 nM) and exhibits an approximately 1370-fold fluorescence enhancement at 39 μM Ca^{2+}. The cell impermeable CaSiR-1 and the cell permeable CaSiR-1AM were used to visualize action-potential-mediated Ca^{2+} in mouse hippocampal CAI pyramidal cells through current stimulation. Near-IR probes can be combined with visible-light emitting probes to monitor different aspects of cellular Ca^{2+} dynamics through multicolor signaling.

While SNAP-tag technology achieves cell localization, near-IR probes have superior optical properties. The combination of these two advances expands the scope of studies possible with Ca^{2+} sensors; however, neither is ideal. SNAP-tag sensors would be improved with more dramatic emission enhancement, and the current near-IR probes bind more weakly than traditional Ca^{2+} sensors. In addition to improving these technologies independently, combining SNAP-tag targeting with near-IR fluorophores would provide powerful tools that address both photophysical and localizations issues encountered with simple sensors.

K^+ Sensors. Potassium and sodium are the most abundant cellular metal ions. Both ions play important roles including membrane polarization during neurotransmission of electrical impulses, maintenance of osmotic pressure and fluid transport.[21,22] The importance of K^+ homeostasis is exemplified by the correlation between breakdowns in K^+ regulation with epileptic seizures,[23] hypertension,[24] and stroke.[25]

Selectively detecting K^+ over Na^+, or the inverse, remains the most difficult aspect of monovalent metal ion sensor design because of physiological concentrations coupled with similar coordination chemistry. The extracellular [Na^+] and intracellular [K^+] exceed 100 mM, while intracellular [Na^+] and extracellular [K^+] are maintained at approximately 5−10 mM. PBFP, the first biological K^+ probe, is comprised of two benzofuran-phthalate dyads linked by a 1,10-diaza-4,7,13,16-tretraoxacyclooctadecane receptor (Figure 5).[26] PBFP binds K^+ with a log K = 1.1 (K_d = 70 mM) and exhibits a 16-fold fluorescence enhancement; however the Na^+ affinity of log K = 0.58 (K_d = 260 mM) limits its applications.

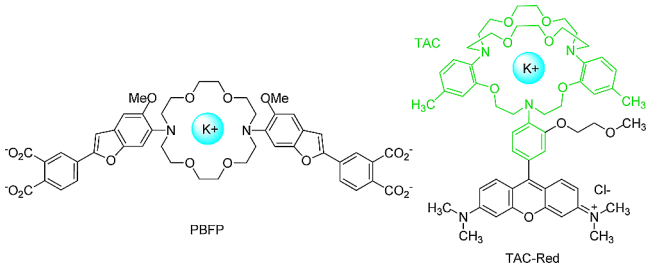

Figure 5. Structure PBFP and TAC-Red showing the binding site for K^+. Coordination of K^+ modulates the fluorescence properties. The TAC receptor (green) in TAC-Red is identical to the ligand used in TAC-Lime and TAC-Crimson, which use different reporting groups.

Cryptand receptors have been explored as an alternative to macrocyclic crown ethers to enhance the selectivity and sensitivity of K^+ probes. The first practical probe incorporated a TAC receptor (2-triazacryptand[2,2.3]-1-(2-methoxyethoxy)-benzene) and a 4-aminonaphthalimide fluorophore on a solid polymer support.[27] While this construct improved K^+ selectivity, only a modest 5.8% fluorescence enhancement was observed in the presence of 2−10 mM K^+. TAC-Red substitutes the napthalimide fluorophore of the first generation probe with a 3,6-bis(dimethylamino)xanthylium fluorophore (Figure 5). TAC-Red exhibits an improved 23-fold emission enhancement over 0−200 mM K^+. The K^+ over Na^+ selectivity (approximately 37-fold) and rapid fluorescence response (<1 ms) enable TAC-Red to image K^+ waves in living mice brain cortex.[28] TAC-Crimson[29] and TAC-Lime$_{dex}$[30] subsequently expanded the scope of K^+-sensitive sensors using the same receptor. TAC-Lime$_{dex}$ utilizes a brighter BODIPY fluorophore and exhibits a 50% fluorescence increase at lower K^+ levels (0−2 mM). The enhanced sensitivity of TAC-Lime$_{dex}$ allowed the identification of electroneutral K^+/Cl^- cotransporter activity in human cervical cancer cells and Ca^{2+}-activated K^+ channels in HT-29 cells involved in K^+ efflux.[30]

Lanthanide-based emission remains underdeveloped in luminescent sensors for metal ions, but Tb-1 demonstrates the potential advantages of these probes.[31] The Tb^{3+}-based detection system contains azaxanthone as a sensitizer, a macrocyclic Tb^{3+} complex as the reporting group and a A_2O_4 (1,10-diaza-4,7,13,16-tretraoxacyclooctadecane) receptor for K^+ (Figure 6). Upon binding K^+, the aryl ether locks the antenna close to the Tb^{3+} center, which enhances energy transfer. K^+ coordination results in a 22-fold luminescence enhancement at λ_{max} 545 nm at 10 mM K^+. Tb-1 binds K^+ with a log K = 6.4 (K_d = 0.33 μM) and exhibits a 93-fold selectivity over Na^+. Since Tb-1 has limited aqueous solubility, Eu-KPhen that uses the same A_2O_4 receptor, a phenanthridine antenna and a macrocyclic europium complex were developed.[32] While aqueous solubility was improved, the lower binding affinity (log K = 4.6, K_d = 26 μM) and decreased luminescence enhancement (2-fold) nullify the advantages of Eu-KPhen over Tb-1. While the early work on lanthanide probes is promising, additional improvements in sensor properties and additional biological studies will need to be conducted to fully evaluate their potential.

Zinc Sensors. Since Zn^{2+}, like Ca^{2+}, is not redox active under physiological conditions, early transport models assumed that proteins acquired Zn^{2+} from a labile cytosolic pool. Recent studies suggest however that cells maintain tight Zn^{2+} homeostasis using metalloregulatory proteins similar to its

dx.doi.org/10.1021/bi3001769 | Biochemistry 2012, 51, 7212−7224

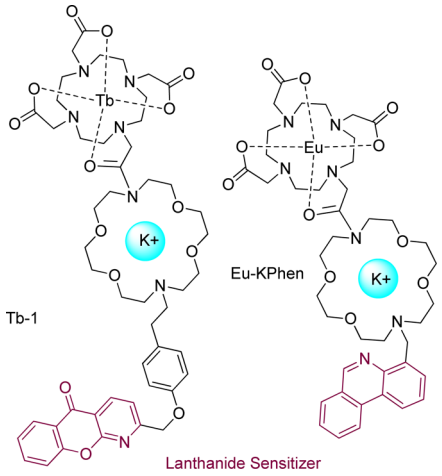

Figure 6. K^+ sensors utilizing lanthanide emission. Both systems utilize an identical macrocyclic K^+ receptor and lanthanide binding group, but different sensitizers (purple) that are tuned to the electronic requirements of Tb^{3+} and Eu^{3+} respectively.

redox active d-block congeners.[33] While [Zn^{2+}] and transport are regulated tightly, Zn^{2+} released from neurons may be involved in signal transduction and excess Zn^{2+} is cytotoxic.[33,34] FluoZin-3 has been used extensively to image Zn^{2+} since it is commercially available.[35] The photophysical properties and preliminary biological imaging studies for numerous Zn^{2+} sensors have been reviewed,[36−40] so the current discussion will highlight recent representative examples.

Over the past decade, Zinpyr sensors have been increasingly popular for studying Zn^{2+} signaling and homeostasis (Figure 7).[41,42] While the first generation compound possesses nanomolar affinity, the second generation ZP1B and ZP3B have micromolar binding affinity and are less sensitive to pH changes.[43] ZPP1, which contains one pyridine and one pyrazine at each Zn^{2+}-binding site, forms a 2:1 M/L complex with log K_1 = 11.2 (K_{d1} = 6.5 pM) and log K_2 = 8.0 (K_{d2} = 9 nM) and exhibits a 13-fold fluorescence enhancement.[44] ZPP1 can detect

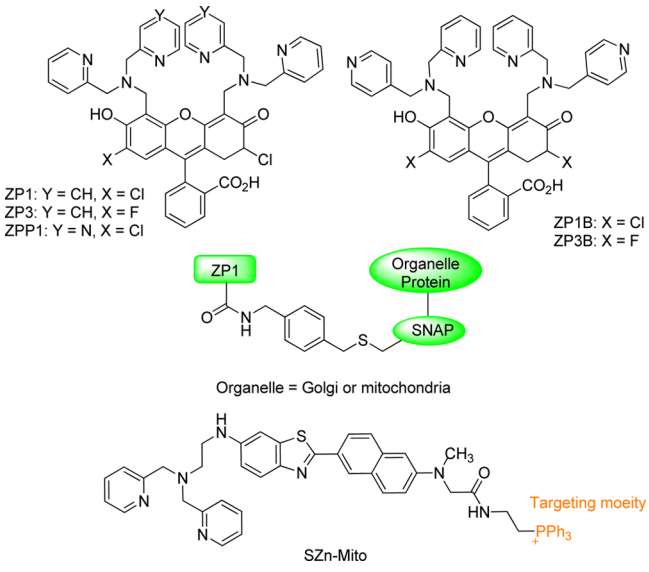

Figure 7. Structure of several Zinpyr sensors and organelle targeted Zn^{2+} probes. The strategy to target Zinpyr sensors to organelles is analogous to the SNAP-tag methodology for Ca^{2+}.

Zn^{2+} released from Min6 cells after stimulation with K^+ and glucose. Like the early Ca^{2+} sensors however, many Zn^{2+} sensors suffer from compartmentalization and heterogeneous distribution in cells. Also like Ca^{2+} sensors, the simple fluorophores can be modified with targeting groups to expand the scope of addressable Zn^{2+} homeostasis questions.

Golgi (pGolgi-AGT) and mitochondria (pMito-AGT) are organelle specific Zn^{2+} probes constructed with a combination of ZP1 and BG like the Ca^{2+} SNAP-tags.[45] SZn-Mito targets the mitochondria utilizing triphenylphosphonium (TPP).[46] SZn-Mito exhibits a slightly improved enhancement of fluorescence compared to pMito-AGT (7- vs 2-fold) and two photon absorption with log K = 8.5 (K_d = 3.1 nM). In studies with rat hippocampal tissue, Zn^{2+} was imaged at a depth of 100−200 μm; however, the response was measured using stimulated Zn^{2+} release. Other targeting strategies have been reported,[47] but all these systems are limited by the properties of the parent sensors. Incorporation of fluorescent sensors with improved binding and fluorescence properties that also include targeting moieties, as well as demonstrated efficacy in imaging Zn^{2+}-based signaling and homeostasis mechanisms, are needed.

Copper Sensors. The reducing environment of the cell renders Cu^+ the predominant form of intracellular copper. While biology exploits Cu redox chemistry to execute important tasks, losing homeostasis has severe consequences. Defects in the metallochaperones that deliver Cu^+ to intracellular targets are hallmarks of Wilson's[48] and Menkes disease,[49] and redox cycling with unregulated Cu^+/Cu^{2+} may be involved in the pathology of neurodegenerative disorders like Parkinson's and prion disease.[50−52] In addition to deleterious effects, recent investigations suggest Cu^+ may have signaling functions like Ca^{2+} and Zn^{2+}.[53,54]

Intracellular Cu^+ can be imaged with techniques like X-ray fluorescence microscopy (XRFM),[55−57] but like measurements of Zn^{2+}, these methods do not differentiate between labile and protein-bound metal ions. Unlike closed shell metal ions, the redox activity of Cu^+ introduces significant obstacles to designing a probe with fluorescence enhancement. Calibrating fluorophore and receptor electronics can circumvent the inherent quenching nature of Cu^+.[58,59] Thioether ligands increase the reduction potential of the bound Cu^+ and inhibit electron transfer to the excited fluorophore, which also can be fine-tuned to energetically isolate the chromophore frontier orbitals from the Cu^+ d electrons.[60]

CTAP-1, the first practical membrane-permeable Cu^+-selective fluorescent sensor integrates a pyrazoline fluorophore and a (1,4,7,10-tetrathia-13-aza)-15-crown-5 receptor (Figure 8).[60] Cu^+-binding enhances fluorescence at λ_{max} 480 nm (4.6-fold). The probe forms a 1:1 metal complex with log K = 10.4 (K_d = 39 pM). Although less sensitive to basal Cu^+, studies using fibroblast cells show that the labile Cu^+ pool predominantly localizes in the mitochondria and GA. Imaging studies with ACu1 confirm the Cu^+ organelle localization. ACu1 is a two photon fluorescent probe composed of a 2-methylamino-6-acetylnaphthalene fluorophore and BETA receptor (bis{2-[2-(2-ethylthio)ethylthio]ethyl}amine).[61] ACu1 exhibits a 4-fold two photon excited fluorescence enhancement and a log K = 10.7 (K_d = 20 pM). In addition to detecting Cu^+ in isolated cells, the probe can also image Cu^+ in hippocampal slices at 90−220 μm depth. CTAP-2, a higher affinity probe with log K = 11.4 (K_d = 4 pM), exhibits 65-fold fluorescence enhancement.[62] CTAP-2 extracts Cu^+ from the chaperone protein Atox1 since the metal site is accessible, but

dx.doi.org/10.1021/bi3001769 | Biochemistry 2012, 51, 7212−7224

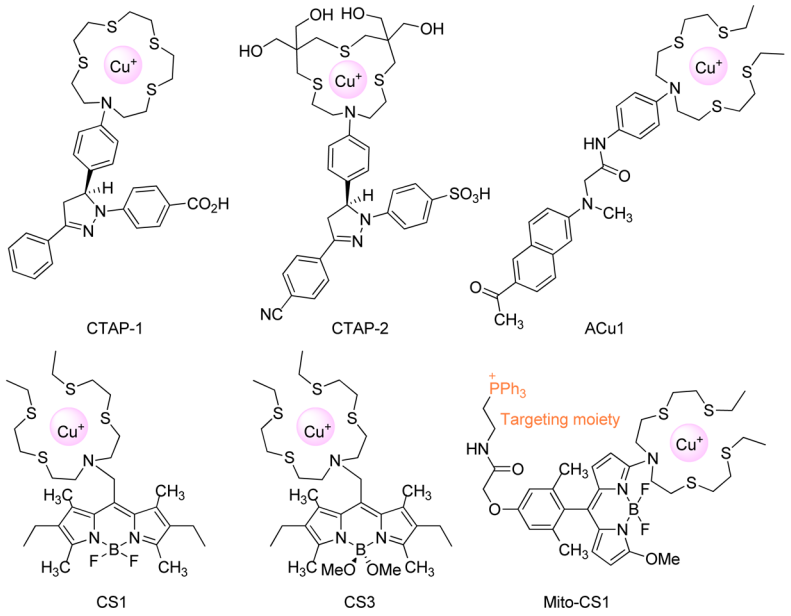

Figure 8. Structures of fluorescent sensors for Cu^+ showing the metal binding site. Mito-CS1 utilizes a TPP group, which is also found in SZn-Mito, to target the mitochondria.

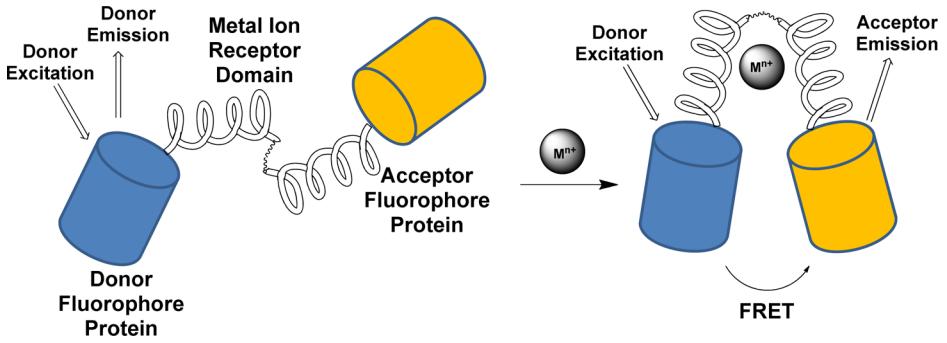

Figure 9. General approach to constructing GFP-based protein sensors. Two GFP-derived proteins that emit at different wavelengths are linked by a metal binding domain that specifically interacts with the metal ion of interest. The conformational change of the receptor upon metal binding results in an intensity ratio change in the donor and acceptor emission. In the absence of metal ion, the fluorescence will come primarily from the donor fluorophore protein, while FRET will increase the contribution of acceptor emission upon analyte binding. The ratio of donor/acceptor emission can be correlated with the concentration of metal ion of interest.

does not remove Cu^+ from active sites embedded with a protein matrix. Intracellular studies have not been reported.

The membrane permeable CS1 composed of a bis{2-[2-(2-ethylthio)ethylthio]ethyl}amine Cu^+ chelator and a BODIPY reporting group produces a 10-fold fluorescent enhancement and log K = 11.4 (K_d = 3.6 pM).[63] CS1 has a limited ability to detect Cu pools at sub-picomolar basal levels. To overcome this limitation, CS3, which displays a 75-fold fluorescence enhancement and log K = 13.1 (K_d = 89 fM), was designed.[54] The probe was used in conjunction with XRFM to observe translocation of Cu^+ from neuronal cell bodies to the periphery. A ratiometric version of CS1 also has been reported.[64] Recent studies raise concerns about lipophilic probes like CS1 and CTAP-1 forming colloidal particles in aqueous solution,[62] which necessitates additional studies to confirm biological observations and development of new probes less susceptible to these issues.

Like Ca^{2+} and Zn^{2+} fluorescence sensors, the biodistribution of analogous Cu^+ probes cannot be controlled, which presents difficulties in mapping homeostasis pathways. To facilitate studies at the organelle level, Mito-CS1, which integrates CS1 with a TPP moiety that targets mitochondria, was developed.[65] A comparative study on cells and patient fibroblasts suggests that while mitochondria are important reservoirs for Cu^+, homeostasis is still controlled at the cellular level. While only a few targeted Cu^+ probes have been reported, the roadmap provided by the Ca^{2+} sensors suggests future development of these sensors would be valuable.

PROTEIN SENSORS

Small molecule fluorescent sensors have facilitated the rapid interrogation of metal ion homeostasis since they are relatively easy to design and implement; however, these tools often suffer from uneven probe biodistribution, sequestration or trapping, cell permeability and cellular toxicity as well as photochemical issues such as bleaching that must be factored into data analysis. Protein-based sensors provide an alternative for monitoring metal ion homeostasis and share the same binding and photochemical requirements of small molecule fluorescent sensors. While some early probes integrate traditional organic fluorophores into biomacromolecules,[66−73] green fluorescent

dx.doi.org/10.1021/bi3001769 | *Biochemistry* 2012, 51, 7212−7224

protein (GFP) and its analogues have become the preferred sensor components.[74,75]

GFP-based metal ion sensors consist of an analyte receptor domain positioned between two proteins that undergo Förster or fluorescence resonance energy transfer (FRET, Figure 9). FRET involves distant-dependent transfer of excitation energy between appropriately matched reporting groups. In protein sensors, metal binding induces conformational changes that are transduced into changes in FRET efficiency. Practically, the ratio of fluorescence emission intensity at two different wavelengths correlates with metal ion concentration. While probe development requires significant time investment to achieve the desired results, genetically encoded probes can target specific organelles or tissues, can be introduced in the cells by transfection and allow long-term imaging because of superior retention.

GFP emission also can be modulated by grafting receptor proteins to the GFP scaffold. In these circularly permeated GFPs, metal ion binding increases fluorescence emission by inducing protein conformational changes, which in turn modulates solvent-fluorophore interactions.[76,77] Although recent efforts have significantly improved the properties of these systems,[78,79] this technique has yet to receive significant attention outside of Ca^{2+} sensing.[80] Opportunities exist for expanding the scope of protein sensors that utilize the circular permutation method.

Calcium Probes. Ca^{2+} was the first metal ion to receive attention in the development of genetically encoded protein probes. In 1997, cameleon Ca^{2+} sensors were developed using FRET as the signaling mechanism.[81] The indicator construction involves the fusion of enhanced blue fluorescent protein (EBFP) or enhanced cyano fluorescent protein (ECFP) mutant of the GFP, calmodulin (CaM), the CaM-binding peptide of skeletal muscle myosin light chain kinase, and the enhanced green or yellow fluorescent protein (EGFP or EYFP). Excitation of ECFP at 440 nm usually results in emission at λ_{max} 480 nm, but when ECFP and EYFP are in close proximity, FRET between ECFP and EYFP results in emission at λ_{max} 545 nm. Ca^{2+} binding to the sensor CaM domain causes the protein conformational change that increases FRET.

When targeted to endoplasmic reticulum (ER) of Hela cells, the yellow cameleons (YCs) indicate $[Ca^{2+}]_{ER}$ homeostasis ranges from 60 to 400 μM at rest to 1−50 μM following Ca^{2+} mobilization; however, the yellow fluorescent protein (YFP) quenching at pH below 7 could limit its utility.[81] The second generation of the cameleon indicators introduced mutations into the acceptor YFP that decreased pH sensitivity, but impaired protein folding.[82] In the third generation cameleon probes, additional mutations provided a pH insensitive probe that folded properly.[83]

Split-YC7.3er, a modified cameleon probe, binds Ca^{2+}, log K = 3.9 (K_d = 130 μM), and detects $[Ca^{2+}]_{ER}$ in Hela cells.[84] Split-YC7.3er measurements coupled with imaging using a small molecule Ca^{2+} sensor to measure cytosolic Ca^{2+} ($[Ca^{2+}]_{cyt}$) show that histamine induced $[Ca^{2+}]_{cyt}$ increases as $[Ca^{2+}]_{ER}$ decreased. Additional measurements of mitochondrial Ca^{2+} ($[Ca^{2+}]_{mt}$) with a third targeted sensor show that $[Ca^{2+}]_{cyt}$ decreases as $[Ca^{2+}]_{mt}$ increases. The combination of these probes demonstrates homeostasis pathways where Ca^{2+} is shuttled from ER into the mitochondria. Although cameleon probes have been encoded in different organelles, introduction to the plasma membrane of neurons remains difficult because of binding interactions with endogeneous CaM.

To address interference with endogenous CaM, the probe/wild-type CaM, (D-family) (D1-D4) Ca^{2+} indicators have been developed by reengineering the binding interface between CaM and the target peptide.[85] The probes are not affected by excess CaM and have been targeted to plasma membrane of hippocampal neurons and the mitochondria. D1 that targets ER (D1ER), binds Ca^{2+} weakly with log K = 3.2 (K_d = 69 μM).[86] D1ER has been used to elucidate the link between familial Alzheimer disease and Ca^{2+} dysregulation in ER.[87] D3 that targets plasma membranes (D3cpV) has better ratiometric sensitivity and has been used to detect Ca^{2+} changes associated with single action potentials in hippocampal neurons, cultured brain cells, and pyramidal cells of living mice using two-photon imaging.[88]

Elimination of wild-type CaM interference also can be achieved by substituting CaM with TnC (troponin C), the calcium regulatory protein found in cardiac and skeletal muscles. Deletion of 14 amino acids from the N terminus of chicken skeletal muscle troponin C (csTnC) followed by sandwiching between CFP and citrine generates TN-L15. The analogous TN-humTnC probe utilizes the human cardiac muscle troponin C (humTnC) instead of csTnC.[89] TN-L15 and TN-humTnC bind Ca^{2+} with log K = 5.9 (K_d = 1.2 μM) and log K = 6.3 (K_d = 470 nM) in vitro and exhibit a fluorescence ratio change of up to 1.4- and 1.7-fold, respectively. TN-L15 localized on the plasma membrane of HEK293 cells and hippocampal neurons reveals that there is no permanent gradient in $[Ca^{2+}]$ from the membrane toward the cytosol. Additional variants adapt the selectivity and affinity properties of these protein sensors for specific applications.[90−92]

Zinc Probes. Using the Ca^{2+} probe model, a Cu^{+} sensor based on the strong interaction between Atox1 copper chaperone and the fourth domain of WD4 (Wilson's disease protein) was designed.[93] Despite using a Cu^{+}-selective protein receptor, the two proteins domains dimerized in the presence of Zn^{2+} with sub-nanomolar affinity, although with a smaller fluorescence ratio change than desirable. The affinity of this probe was broadened to the pM-fM range by fusing the two sensing domains with variable peptide linkers generating CFP-Atox1-linker-WD4-YFP (CALWY) Zn^{2+} probes.[94] Subsequently, replacing ECFP and EYFP with cerulean and citrine generates enhanced CALWY (eCALWY) with improved emission ratio changes.[95] The eCALWY series of probes (eCALWY-1 to -6) bind Zn^{2+} in the pM-nM range and exhibit an approximately 2-fold fluorescence ratio change. eCALWY-1 reveals chelatable cytosolic Zn^{2+} (approximately 0.4 nM) in pancreatic ß cell and higher levels in insulin-containing secretory vesicles. Additional related probes were developed but not applied to cellular studies.[93,96,97]

Classical Cys_2His_2 zinc fingers are held together by Zn^{2+} inducing a globular, compact protein structure. To take advantage of the structural motif in sensing, the zinc finger sequence from mammalian transcription factor Zif268 has been utilized in probes that target organelles. The Cys_2His_2 version of the sensor was targeted to cytosol and mitochondria, while the His_4 probe was targeted to plasma membrane.[98] Cys_2His_2 and His_4 sensors bind to intracellular Zn^{2+} with log K = 5.8 (K_d = 1.5 μM) and log K = 3.6 (K_d = 200 μM) respectively with a minimal emission ratio change of 0.25-fold as compared to 2.2−4-fold observed in in vitro measurements respectively. Measurements with the Cys_2His_2 sensor suggest that the resting cytosolic $[Zn^{2+}]$ is 180 nM while that of mitochondria is 680

dx.doi.org/10.1021/bi3001769 | Biochemistry 2012, 51, 7212−7224

nM in mammalian cells; however, this value was extrapolated using the weakly binding probe. Studies with Cys_2His_2 in rat hippocampal neurons demonstrate mitochondria act as a Zn^{2+} reservoir and source in a Ca^{2+}-dependent manner.

Zap1, the zinc-responsive transcriptional activator, contains two zinc fingers of high Zn^{2+} affinity log $K \approx 9.7$ ($K_d \approx 0.2$ nM).[99] The Zn^{2+} complex forms from an interacting finger-pair structure.[100,101] To optimize the Zn^{2+}affinity, Zap1 was placed between truncated CFP and citrine generating the ZapCY1 sensor.[102] ZapCY1 bind Zn^{2+} with a high affinity in vitro log K = 11.6 (K_d = 2.5 pM) and exhibits a 4.1-fold emission ratio change. Mutating two cysteines in the binding domain of ZapCY1 generates ZapCY2 that binds Zn^{2+} with a lower affinity, log K = 9.1 (K_d = 811 pM) and exhibits a 1.4-fold emission ratio change. Measurements with ZapCY2 reveal 80 pM free Zn^{2+} in HeLa cell cytosol in contrast to the 180 nM value obtained previously,[98] but consistent with the new sensor's ability to more accurately measure lower basal levels and in reasonable agreement with analogous studies conducted with eCALWY probes.[95]

When ZapCY1 was targeted to ER and Golgi apparatus (GA), the resting $[Zn^{2+}]_{ER}$ and $[Zn^{2+}]_{Golgi}$ were measured at 0.9 and 0.6 pM respectively. Elevated cytosolic Zn^{2+} was sequested into ER and GA in a Ca^{2+} dependent manner. To further probe Ca^{2+}dependence, D1ER[86] and D3cpv[88] were incorporated into the cell as well. The measurements reveal that elevated $[Ca^{2+}]_{cyto}$ induces Zn^{2+} efflux from the ER, while elevated $[Zn^{2+}]_{cyto}$ induces Ca^{2+} release from the ER. This indicates the possibility of Ca^{2+}-dependent Zn^{2+} homeostasis. Furthermore, the studies demonstrate the ability to monitor complex homeostasis pathways using multiple genetically encoded protein sensors, which is more difficult to achieve using small molecule fluorescent sensors.

Copper Probes. Amt-1, a Cu^+ dependent regulator in *Candida glabrata*, detects high levels of copper and consequently stimulates Cu detoxification genes.[103,104] Amt-1 is unstructured in the absence of Cu^+ but clusters upon Cu^+ binding and undergoes a conformation change. The Cu^+ binding motif of Amt1 (residues 36−110) has been integrated into Amt1-FRET sensor, which uses CFP and YFP.[105] An increase in FRET of 1.9−2.3-fold was observed upon Cu^+ binding (log K = 17.6, K_d = 2.5 aM, attomolar, 10^{-18}). In CHO-K1, measurements with Amt1-FRET suggest the effective labile $[Cu^+]$ of approximately 10 aM, which is consistent with previous studies of metallochaperones.[106,107] To further these studies, Ace1, a homologue of Amt1, and Mac1, a copper dependent regulator that stimulates the copper uptake genes in low copper concentrations,[108] were integrated into Acel-1 FRET and Mac1-FRET.[109] Acel-FRET and Mac1-FRET bind Cu^+ with log K = 17.3 (K_d = 4.7 aM) and log K = 19.0 (K_d = 970 aM) respectively. Using the two sensors simultaneously demonstrated that the yeast cells maintain Cu^+ homeostasis between approximately 89 aM and 5.1 zM (10^{-21}). A wider range of genetically encoded Cu^+ and Zn^{2+} probes are still needed, but the cell studies reported to date support the hypothesis that the homeostasis of these metal ions is highly controlled.

PHOTOCAGED COMPLEXES

Small molecule and protein sensors can image endogenous metal ions, but correlating metal ion concentrations to physiological phenomena can be difficult using fluorescence alone. Determining cellular responses to an added metal ion can complement the information acquired with sensors to provide a more complete picture. Solutions of metal salts can be applied to cells either with or without a chelator to act as a metal ion buffer. While potentially useful, these approaches cannot provide temporal or spatial control over metal ion release, relying on diffusion as the primary mode of transport, and on the response time of the individual adding the solution and executing the experiment.

Alternatively, photocaged complexes provide an approach that circumvents the limitations of working with metal ion buffers. Photocaged complexes bind a metal ion until a light-induced chemical reaction releases the analyte. Unlike fluorescent sensors, photocaged complexes need not exhibit absolute binding specificity provided the exchange rate with competing metal ions remains slow. Photocaged complexes must possess a metal ion affinity high enough to prevent proteins from scavenging the metal ion and perturbing homeostasis prior to photo-uncaging; in addition, photo-products should have lower affinity than the biological receptors being investigated and release the metal ion quickly after photo-uncaging. Since metal ion release involves the scission of a covalent bond, photo-uncaging typically requires high energy, near UV light, so high quantum yields are preferable.

Calcium Photocages. Although Ca^{2+} fluorescent sensors significantly advanced the understanding of intracellular signaling pathways, correlating concentration fluctuations directly with biological events remained challenging. The concurrent development of two strategies for releasing Ca^{2+} from chelating ligands overcame these obstacles. Both photocaged Ca^{2+} complex designs exploited a nitrobenzyl photoactive group, but each used a different release mechanism. In the first as exemplified by Nitr-5, photolysis modulates the electron donating ability of a Ca^{2+}-bound aniline nitrogen atom, which attenuates binding affinity (Figure 10).[110] In contrast,

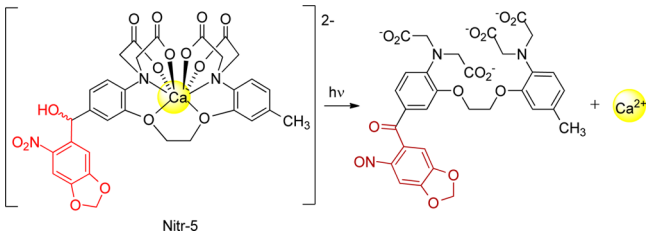

Figure 10. Structure and uncaging mechanism of the Ca^{2+} photocage Nitr-5. Exposure to light induces transformation nitrobenzhydrol group (red) into a nitrosobenzophenone (dark red). The introduction of an electron drawing group *para* to the metal ion-bound aniline nitrogen atom weakens binding affinity of the receptor, which increases the availability of labile Ca^{2+}.

the second strategy involves a light initiated bond cleavage reaction, which fractures the chelator into two fragments releasing the bound Ca^{2+} (Figure 11).[111,112] Several of these calcium photocages are commercially available and have been used extensively to investigate signaling and homeostasis.

Calcium photo-uncaging using DM-Nitrophen, a photocage that utilizes an EDTA-based (ethylenediaminetetraacetic acid) chelator, has found wide application in studying Ca^{2+} homeostasis and signaling. Ca^{2+} photo-uncaging has been used to study release of neurotransmitters in relation to Ca^{2+} channels,[113] potentiators[114,115] and recruitment of releasable vesicle in calyx-of-Held synapses.[116,117] In cardiac myocytes,

dx.doi.org/10.1021/bi3001769 | *Biochemistry* 2012, 51, 7212−7224

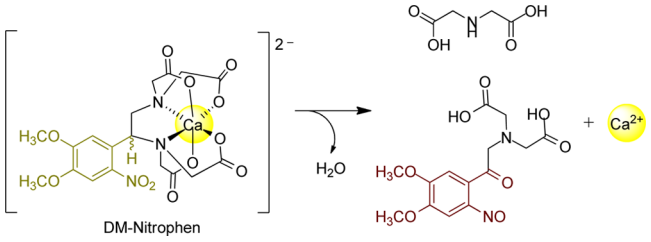

Figure 11. Structure and uncaging mechanism of the Ca^{2+} photocage DM-Nitrophen. Irradiation of the nitrobenzyl group with light results in the scission of a carbon−nitrogen bond, which bifurcates the receptor. The reduction in the chelate effect shifts the equilibrium of Ca^{2+} binding toward free (aqua) metal ion.

DM-Nitrophen has been used to elucidate the turnover rate of the functional Na^+-Ca^{2+} exchanger[118] and to study vasodilation and vasoconstriction in astrocytes.[119,120] Although DM-nitrophen binds Ca^{2+} with log K = 8.3 (K_d = 5 nM, $\Phi_{photolysis}$ = 0.23), the Mg^{2+} with log K = 5.6 (K_d = 2.5 μM) becomes problematic when [Mg^{2+}] is high. Since the normal resting [Mg^{2+}] is approximately 1 mM, DM-nitrophen will be largely bound to Mg^{2+} ions unless studies are conducted under Mg^{2+} deplete conditions.

The NP-EGTA photocage based on an ethylene glycol-bis(2-aminoethylether)-*N*,*N*,*N*′,*N*′-tetraacetic acid (EGTA) chelator binds Ca^{2+} with log K = 7.1 (K_d = 80 nM, $\Phi_{photolysis}$ = 0.23) and a Mg^{2+} with log K = 2.0 (K_d = 9.0 mM), which overcomes the selectivity problems (Figure 12). Flash photolysis studies using

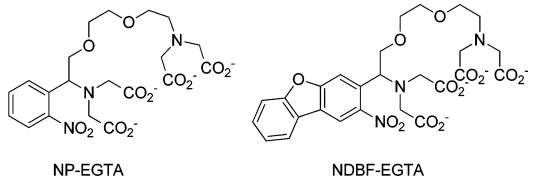

Figure 12. Additional Ca^{2+} photocages that utilize the same uncaging mechanism as DM-Nitrophen. NDBF-EGTA has the additional advantage of sensitivity to two-photon excitation.

NP-EGTA have shown that intracellular calcium levels modulate fast and slow endocytosis at synapses,[121] the size of releasable vesicle pools[122] and the vesicle release rate at phasic boutons.[123] In astrocytes, NP-EGTA photolysis has been used to examine the relationship between astrocytic internal Ca^{2+} levels and Ca^{2+}-dependent glutamate release,[124] and for the study of Ca^{2+} requirements in long-term synaptic depression.[122]

In biological studies, the use of near-UV light to initiate metal ion release can induce cell damage and viability issues, so Ca^{2+} photocages with large TPCS (two-photon cross sections) are desirable. Typically nitrobenzyl and dimethoxynitrobenzyl photocaging groups exhibit low photolysis quantum yields with two-photo absorption (TPA). In TPA, two lower energy photons are absorbed simultaneously to populate the excited state usually reached using higher energy light.[125,126] Two-photon techniques also can be focused to a small volume (approximately 1 fL) in contrast to one-photon excitation, which occurs over a wider area,[127] and allows photo-uncaging several hundred μm deep in tissues.[128]

While DM-nitrophen has a TPA of 0.01−0.04 GM (Göppert-Mayer), the related photocage NDBF-EGTA that utilizes a nitrodibenzofuran photocaging group has a large TPCS 0.6 GM. NDBF-EGTA binds Ca^{2+} with log K = 7 (K_d = 100 nM) and $\Phi_{photolysis}$ = 0.7.[129] NDBF-EGTA in combination with the Ca^{2+} sensor Fluo-3 showed release of photocaged Ca^{2+} on the surface of the sarcoplasmic reticulum induced additional localized Ca^{2+} release in cardiac myocytes. Compared to the TPCS of some chromophores, the photophysical properties of TPA photocaged complexes could still be improved.

Zinc Photocages. Zn has been implicated in neurotransmission; however, exact signaling mechanisms have yet to be elucidated fully. Proteins including metallothioneins help maintain Zn^{2+} homeostasis, and Zn^{2+} release from these proteins may be involved in protecting cells from oxidative stress.[130] To facilitate Zn^{2+} signaling and homeostasis research, we have developed Zn^{2+} photocages employing strategies similar to those employed for Ca^{2+}. ZinCast-1 utilizes a dipicolylanilino ligand for Zn^{2+} (Figure 13)[131] and has a metal

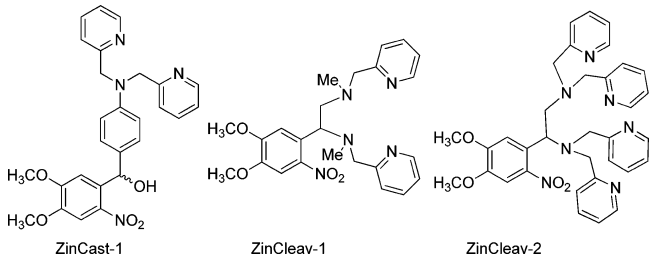

Figure 13. Zn^{2+} photocages. ZinCast-1 utilizes the Nitr-5 metal ion release strategy and the ZinCleav compounds follow the DM-Nitrophen model.

ion release mechanism similar to Nitr-5. ZinCast-1 binds Zn^{2+} with log K = 4.8 (K_d = 14.3 μM) while ZinUnc-1 has a lower affinity (log K = 2.2, K_d = 5.5 mM). ZinCast-1 and [Zn(ZinCast-1)]$^{2+}$ uncage with photolysis quantum yields of 0.7 and 1.0% respectively. The affinity for Zn^{2+} drops over 2 orders of magnitude after photo-uncaging (ΔK_d = $K_{d\text{-Uncaged}}$/$K_{d\text{-Caged}}$). Work with ZinCast-1 illustrates the challenges in using this class of photocages for biological investigations. While the ΔK_d is reasonable for some applications, the relatively weakly binding photocage would likely perturb homeostasis prior to photolysis if the Zn^{2+} complex was introduced to cells. In contrast, the photocage Nitr-5 can effectively sequester Ca^{2+}, but the uncaged ligand retains a high affinity for the metal ion, which limits Ca^{2+} concentrations perturbations. Further studies with related benzhydrol-based metal ion photocages suggest that the ligand design inhibits photo-uncaging, which limits the maximum release efficiency achievable.[132−134]

ZinCleav-1 takes advantage of a similar bond cleavage strategy to DM-Nitrophen (Figure 11), and unlike ZinCast-1 utilizes aliphatic amines in the tetradentate ligand EBAP (ethylene-bis-α,α′-(2-aminomethyl)pyridine), which greatly improves binding affinity (log K = 12.6, K_d = 0.23 pM).[135] Upon irradiation of [Zn(ZnCleav-1)]$^{2+}$ with 350 nm light, bond cleavage generates two weakly Zn^{2+}-binding 2-(aminomethyl)pyridine fragments, which releases the bound metal ion. The $\Phi_{photolysis}$ of ZinCleav-1 and [Zn(ZnCleav-1)]$^{2+}$ is 2.2% and 1.7% respectively, and the ΔK_d is significantly greater than ZinCast-1. In many cell types however, Zn^{2+}-binding proteins could scavenge Zn^{2+} from [Zn(ZnCleav-1)]$^{2+}$ prior to photo-uncaging.

The second generation photocage, ZinCleav-2 utilizes the hexadentate TPEN (*N*,*N*,*N*′,*N*′-tetrakis(2-pyridylmethyl)-ethylenediamine) receptor,[136] which possesses a higher affinity for

dx.doi.org/10.1021/bi3001769 | *Biochemistry* 2012, 51, 7212−7224

Zn^{2+} (log K = 15.4, K_d = 0.4 fM), which is higher affinity than most metalloproteins. ZinCleav-2 binds Zn^{2+} more tightly than ZinCleav-1 with log K = 15.0 (K_d = 0.9 fM) and a ΔK_d after photo-uncaging of $>10^8$ at pH 7.4. The $\Phi_{photolysis}$ of ZinCleav-2 and $[Zn(ZnCleav\text{-}2)]^{2+}$ are 4.7% and 2.3% respectively. These preliminary results are promising and biological studies are being pursued.

Copper Photocages. While the first Cu^+ photocage has only recently been reported,[137] several Cu^{2+} systems have been characterized (Figure 14). The Cu^{2+} photocage Cucage

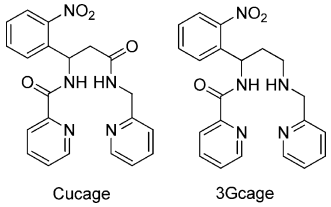

Figure 14. Photocages for Cu^{2+}. Cucage and 3Gcage utilize the DM-Nitrophen uncaging strategy and have been used to generate reactive oxygen species in biological assays.

incorporates a bispyridylamide chelator and releases the metal ion by a similar mechanism to ZinCleav and DM-Nitrophen.[138] At pH 7.4, H_2cage binds Cu^{2+} to form $[Cu(OH_2)(Cucage)]$ complex with a log K = 10.7 (K_d = 16 pM). Upon photolysis, bidentate photoproducts with reduced affinity for Cu^{2+} are formed; in addition, Cucage has been utilized as a Pt^{2+} photocage.[139] A binding affinity of 16 pM is not sufficient to keep copper sequestered in the cell prior to photo-uncaging since cells maintain [Cu] at < fM. 3Gcage with improved Cu^{2+} binding properties was developed as potential oxidative stress-induced prodrug.[140] 3Gcage has high affinity (log K = 15.7, K_d = 0.18 fM). In vitro studies with both Cucage and 3Gcage showed Cu^{2+} release from both increased hydroxyl radical formation through Fenton-like chemistry as indicated by deoxyribose degradation assays. While Cu^+ is not the mobile form of Cu in biology, future studies with these photocages could help illuminate how reactive oxygen species damage cells.

PROSPECTS

The last 30 years have seen an increased interest in metal ion signaling and homeostasis as well as the techniques to study these important biological phenomena. Studies using a variety of photochemical tools have been pivotal in establishing the signaling functions of Ca^{2+}. Recent efforts are seeking to follow a similar approach to understand the biology of Zn^{2+} and Cu^+. Since the homeostasis of Zn^{2+} and Cu^+ is tightly regulated, an array of sensors and photocages with different metal binding properties will be required to probe homeostasis in different types of cells. Loss of homeostasis associated with disease states and localized concentrations of labile metal ions increase the need for and opportunities to develop specially engineered photochemical tools for Zn^{2+} and Cu^+. In addition to Zn^{2+} and Cu^+, there are significant opportunities to develop photochemical tools for important metal ions like Fe^{2+}/Fe^{3+}, Cu^{2+}, Ni^{2+} and K^+ that have received less attention to date. While some of these metal ions like Ni^{2+} have been the subject of the development of small molecule[141] and protein-based sensors,[142] the need for more and better photochemical tools is imperative.

AUTHOR INFORMATION

Corresponding Author

*E-mail: scburdette@wpi.edu. Telephone (508) 831-5224.

Funding

Research in our laboratory is funded by the Worcester Polytechnic Institute and NSF grants CHE-0955361 and CHE-1012905.

Notes

The authors declare no competing financial interest.

ABBREVIATIONS USED

A_2O_4, 1,10-diaza-4,7,13,16-tetraoxacyclooctadecane; aM, atto-molar; BAPTA, 1,2-bis(*o*-aminophenoxy)ethane-*N*,*N*,*N*′,*N*′-tetraacetic acid; BETA, bis{2-[2-(2-ethylthio)ethylthio]ethyl}-amine; BG, O^6-benzylguanine; BODIPY, boron-dipyrromethene; CALWY, CFP-Atox1-linker-WD4-YFP; CaM, calmodulin; csTnC, chicken skeletal muscle troponin; EBAP, ethylene-bis-α,α'-(2-aminomethyl)pyridine; EBFP, enhanced blue fluorescent protein; eCALWY, enhanced CALWY; ECFP, cyano fluorescent protein; EYFP, enhanced yellow fluorescent protein; EDTA, ethylenediaminetetraacetic acid; EGTA, ethylene glycol-bis(2-aminoethylether)-*N*,*N*,*N*′,*N*′-tetraacetic acid; ER, endoplasmic reticulum; FRET, Förster or fluorescence resonance energy transfer; GA, Golgi apparatus; GFP, green fluorescent protein; GM, Göppert-Mayer; humTnC, human cardiac muscle troponin C; PBFP, potassium binding benzofuran phthalate; TAC, 2-triazacryptand[2,2.3]-1-(2-methoxyethoxy) benzene; TnC, troponin C; TPA, two-photo absorption; TPCS, two-photon cross-section; TPEN, *N*,*N*,*N*′,*N*′-tetrakis(2-pyridylmethyl)-ethylenediamine; TPP, triphenylphosphonium; WD4, Wilson's disease protein; YC, yellow cameleons; XRFM, X-ray fluorescence microscopy

REFERENCES

(1) Pantopoulos, K., Porwal, S. K., Tartakoff, A., and Devireddy, L. (2012) Mechanisms of Mammalian Iron Homeostasis. *Biochemistry 51*, 5705−5724.

(2) Kaplan, C. D., and Kaplan, J. (2009) Iron Acquisition and Transcriptional Regulation. *Chem. Rev. 109*, 4536−4552.

(3) Tiffany-Castiglioni, E., Hong, S., and Qian, Y. (2011) Copper Handling by Astrocytes: Insights into Neurodegenerative Diseases. *Int. J. Dev. Neurosci. 29*, 811−818.

(4) Tsien, R. (1989) Fluorescent-Probes of Cell Signaling. *Annu. Rev. Neurosci. 12*, 227−253.

(5) de Silva, A. P., Gunaratne, H. Q. N., Gunnlaugsson, T., Huxley, A. J. M., McCoy, C. P., Rademacher, J. T., and Rice, T. E. (1997) Signaling Recognition Events with Fluorescent Sensors and Switches. *Chem. Rev. 97*, 1515−1566.

(6) Chang, W., and Shoback, D. (2004) Extracellular Ca^{2+}-Sensing Receptors - an Overview. *Cell Calcium. 35*, 183−196.

(7) Ritchie, M. F., Zhou, Y., and Soboloff, J. (2011) Transcriptional Mechanisms Regulating Ca^{2+} Homeostasis. *Cell Calcium 49*, 314−321.

(8) Trump, B., and Berezesky, I. (1995) Calcium-Mediated Cell Injury and Cell Death. *FASEB J. 9*, 219−228.

(9) Gee, K. R., Brown, K. A., Chen, W. N. U., Bishop-Stewart, J., Gray, D., and Johnson, I. (2000) Chemical and Physiological Characterization of Fluo-4 Ca^{2+}-Indicator Dyes. *Cell Calcium. 27*, 97−106.

(10) Grynkiewicz, G., Poenie, M., and Tsien, R. Y. (1985) A New Generation of Ca^{2+} Indicators with Greatly Improved Fluorescence Properties. *J. Biol. Chem. 260*, 3440−3450.

(11) Allbritton, N. L., Oancea, E., Kuhn, M. A., and Meyer, T. (1994) Source of Nuclear Calcium Signals. *Proc. Natl. Acad. Sci. U. S. A. 91*, 12458−12462.

(12) Sanchez-Martin, R. M., Cuttle, M., Mittoo, S., and Bradley, M. (2006) Microsphere-Based Real-Time Calcium Sensing. *Angew. Chem., Int. Ed. 45*, 5472−5474.
(13) Keppler, A., Gendreizig, S., Gronemeyer, T., Pick, H., Vogel, H., and Johnsson, K. (2003) A General Method for the Covalent Labeling of Fusion Proteins with Small Molecules in Vivo. *Nat. Biotechnol. 21*, 86−89.
(14) Gronemeyer, T., Chidley, C., Juillerat, A., Heinis, C., and Johnsson, K. (2006) Directed Evolution of O^6-Alkylguanine-DNA Alkyltransferase for Applications in Protein Labeling. *Protein Eng. Des. Sel. 19*, 309−316.
(15) Kamiya, M., and Johnsson, K. (2010) Localizable and Highly Sensitive Calcium Indicator Based on a BODIPY Fluorophore. *Anal. Chem. 82*, 6472−6479.
(16) Bannwarth, M., Corrêa, I. R., Sztretye, M., Pouvreau, S., Fellay, C., Aebischer, A., Royer, L., Ríos, E., and Johnsson, K. (2009) Indo-1 Derivatives for Local Calcium Sensing. *ACS Chem. Biol. 4*, 179−190.
(17) Palmer, A. E. (2009) Expanding the Repertoire of Fluorescent Calcium Sensors. *ACS Chem. Biol. 4*, 157−159.
(18) Matsui, A., Umezawa, K., Shindo, Y., Fujii, T., Citterio, D., Oka, K., and Suzuki, K. (2011) A Near-Infrared Fluorescent Calcium Probe: A New Tool for Intracellular Multicolour Ca^{2+} Imaging. *Chem. Commun. 47*, 10407−10409.
(19) Umezawa, K., Matsui, A., Nakamura, Y., Citterio, D., and Suzuki, K. (2009) Bright, Color-Tunable Fluorescent Dyes in the Vis/NIR Region: Establishment of New "Tailor-made" Multicolor Fluorophores Based on Borondipyrromethene. *Chem.—Eur. J. 15*, 1096−1106.
(20) Egawa, T., Hanaoka, K., Koide, Y., Ujita, S., Takahashi, N., Ikegaya, Y., Matsuki, N., Terai, T., Ueno, T., Komatsu, T., and Nagano, T. (2011) Development of a Far-Red to Near-Infrared Fluorescence Probe for Calcium Ion and its Application to Multicolor Neuronal Imaging. *J. Am. Chem. Soc. 133*, 14157−14159.
(21) Kress, G. J., and Mennerick, S. (2009) Action Potential Initiation and Propagation: Upstream Influences on Neurotransmission. *Neuroscience. 158*, 211−222.
(22) Catterall, W. A. (2010) Ion Channel Voltage Sensors: Structure, Function, and Pathophysiology. *Neuron. 67*, 915−928.
(23) Froehlich, F., Bazhenov, M., Iragui-Madoz, V., and Sejnowski, T. J. (2008) Potassium Dynamics in the Epileptic Cortex: New Insights on an Old Topic. *Neuroscientist. 14*, 422−433.
(24) Holtzclaw, J. D., Grimm, P. R., and Sansom, S. C. (2011) Role of BK Channels in Hypertension and Potassium Secretion. *Curr. Opin. Nephrol. Hypertens. 20*, 512−517.
(25) Baczko, I., Husti, Z., Lang, V., Lepran, I., and Light, P. E. (2011) Sarcolemmal K(ATP) Channel Modulators and Cardiac Arrhythmias. *Curr. Med. Chem. 18*, 3640−3661.
(26) Minta, A., and Tsien, R. Y. (1989) Fluorescent Indicators for Cytosolic Sodium. *J. Biol. Chem. 264*, 19449−19457.
(27) He, H., Mortellaro, M. A., Leiner, M. J. P., Fraatz, R. J., and Tusa, J. K. (2003) A Fluorescent Sensor with High Selectivity and Sensitivity for Potassium in Water. *J. Am. Chem. Soc. 125*, 1468−1469.
(28) Padmawar, P., Yao, X., Bloch, O., Manley, G. T., and Verkman, A. S. (2005) K^+ Waves in Brain Cortex Visualized using a Long-Wavelength K^+-Sensing Fluorescent Indicator. *Nature Methods. 2*, 825−827.
(29) Magzoub, M., Padmawar, P., Dix, J. A., and Verkman, A. S. (2006) Millisecond Association Kinetics of K^+ with Triazacryptand-Based K^+ Indicators Measured by Fluorescence Correlation Spectroscopy. *J. Phys. Chem. B. 110*, 21216−21221.
(30) Namkung, W., Padmawar, P., Mills, A. D., and Verkman, A. S. (2008) Cell-Based Fluorescence Screen for K^+ Channels and Transporters using an Extracellular Triazacryptand-Based K^+ Sensor. *J. Am. Chem. Soc. 130*, 7794−7795.
(31) Thibon, A., and Pierre, V. C. (2008) A Highly Selective Luminescent Sensor for the Time-Gated Detection of Potassium. *J. Am. Chem. Soc. 131*, 434−435.
(32) Weitz, E. A., and Pierre, V. C. (2011) A Ratiometric Probe for the Selective Time-Gated Luminescence Detection of Potassium in Water. *Chem. Commun. 47*, 541−543.
(33) Fukada, T., Yamasaki, S., Nishida, K., Murakami, M., and Hirano, T. (2011) Zinc Homeostasis and Signaling in Health and Diseases. *J. Biol. Inorg. Chem. 16*, 1123−1134.
(34) Colvin, R. A., Holmes, W. R., Fontaine, C. P., and Maret, W. (2010) Cytosolic Zinc Buffering and Muffling: Their Role in Intracellular Zinc Homeostasis. *Metallomics. 2*, 306−317.
(35) Gee, K., Zhou, Z., Qian, W., and Kennedy, R. (2002) Detection and Imaging of Zinc Secretion from Pancreatic Beta-Cells using a New Fluorescent Zinc Indicator. *J. Am. Chem. Soc. 124*, 776−778.
(36) Thompson, R. (2005) Studying Zinc Biology with Fluorescence: Ain't we Got Fun? *Curr. Opin. Chem. Biol. 9*, 526−532.
(37) Terai, T., and Nagano, T. (2008) Fluorescent Probes for Bioimaging Applications. *Curr. Opin. Chem. Biol. 12*, 515−521.
(38) Tomat, E., and Lippard, S. J. (2010) Imaging Mobile Zinc in Biology. *Curr. Opin. Chem. Biol. 14*, 225−230.
(39) Jiang, P., and Guo, Z. (2004) Fluorescent Detection of Zinc in Biological Systems: Recent Development on the Design of Chemosensors and Biosensors. *Coord. Chem. Rev. 248*, 205−229.
(40) Xu, Z., Yoon, J., and Spring, D. R. (2010) Fluorescent Chemosensors for Zn2. *Chem. Soc. Rev. 39*, 1996−2006.
(41) Walkup, G. K., Burdette, S. C., Lippard, S. J., and Tsien, R. Y. (2000) A New Cell-Permeable Fluorescent Probe for Zn^2. *J. Am. Chem. Soc. 122*, 5644−5645.
(42) Burdette, S. C., Walkup, G. K., Spingler, B., Tsien, R. Y., and Lippard, S. J. (2001) Fluorescent Sensors for Zn^{2+} Based on a Fluorescein Platform: Synthesis, Properties and Intracellular Distribution. *J. Am. Chem. Soc. 123*, 7831−7841.
(43) Wong, B. A., Friedle, S., and Lippard, S. J. (2009) Subtle Modification of 2,2-Dipicolylamine Lowers the Affinity and Improves the Turn-on of Zn(II)-Selective Fluorescent Sensors. *Inorg. Chem. 48*, 7009−7011.
(44) Zhang, X., Hayes, D., Smith, S. J., Friedle, S., and Lippard, S. J. (2008) New Strategy for Quantifying Biological Zinc by a Modified Zinpyr Fluorescence Sensor. *J. Am. Chem. Soc. 130*, 15788−15789.
(45) Tomat, E., Nolan, E. M., Jaworski, J., and Lippard, S. J. (2008) Organelle-Specific Zinc Detection using Zinpyr-Labeled Fusion Proteins in Live Cells. *J. Am. Chem. Soc. 130*, 15776−15777.
(46) Masanta, G., Lim, C. S., Kim, H. J., Han, J. H., Kim, H. M., and Cho, B. R. (2011) A Mitochondrial-Targeted Two-Photon Probe for Zinc Ion. *J. Am. Chem. Soc. 133*, 5698−5700.
(47) Iyoshi, S., Taki, M., and Yamamoto, Y. (2011) Development of a Cholesterol-Conjugated Fluorescent Sensor for Site-Specific Detection of Zinc Ion at the Plasma Membrane. *Org. Lett. 13*, 4558−4561.
(48) Ala, A., Walker, A. P., Ashkan, K., Dooley, J. S., and Schilsky, M. L. (2007) Wilson's Disease. *Lancet. 369*, 397−408.
(49) Bertini, I., and Rosato, A. (2008) Menkes Disease. *Cell. Mol. Life Sci. 65*, 89−91.
(50) Brown, D. R., and Kozlowski, H. (2004) Biological Inorganic and Bioinorganic Chemistry of Neurodegeneration Based on Prion and Alzheimer Diseases. *Dalton Trans.*, 1907−1917.
(51) Bush, A. I., Barnham, K. J., and Masters, C. L. (2004) Neurodegenerative Diseases and Oxidative Stress. *Nature Rev. Drug Discovery 3*, 205−214.
(52) Valensin, G., Gaggelli, E., Kozlowski, H., and Valensin, D. (2006) Copper Homeostasis and Neurodegenerative Disorders (Alzheimer's, Prion, and Parkinson's Diseases and Amyotrophic Lateral Sclerosis). *Chem. Rev. 106*, 1995−2044.
(53) Schlief, M., Craig, A., and Gitlin, J. (2005) NMDA Receptor Activation Mediates Copper Homeostasis in Hippocampal Neurons. *J. Neurosci. 25*, 239−246.
(54) Dodani, S. C., Domaille, D. W., Nam, C. I., Miller, E. W., Finney, L. A., Vogt, S., and Chang, C. J. (2011) Calcium-Dependent Copper Redistributions in Neuronal Cells Revealed by a Fluorescent Copper Sensor and X-Ray Fluorescence Microscopy. *Proc. Natl. Acad. Sci. U. S. A. 108*, 5980−5985.
(55) Qin, Z., Caruso, J. A., Lai, B., Matusch, A., and Becker, J. S. (2011) Trace Metal Imaging with High Spatial Resolution: Applications in Biomedicine. *Metallomics. 3*, 28−37.

(56) Fahrni, C. J. (2007) Biological Applications of X-Ray Fluorescence Microscopy: Exploring the Subcellular Topography and Speciation of Transition Metals. *Curr. Opin. Chem. Biol. 11*, 121−127.
(57) McRae, R., Bagchi, P., Sumalekshmy, S., and Fahrni, C. J. (2009) In Situ Imaging of Metals in Cells and Tissues. *Chem. Rev. 109*, 4780−4827.
(58) Que, E. L., Domaille, D. W., and Chang, C. J. (2008) Metals in Neurobiology: Probing their Chemistry and Biology with Molecular Imaging. *Chem. Rev. 108*, 1517−1549.
(59) Domaille, D. W., Que, E. L., and Chang, C. J. (2008) Synthetic Fluorescent Sensors for Studying the Cell Biology of Metals. *Nat. Chem. Biol. 4*, 168−175.
(60) Yang, L., McRae, R., Henary, M. M., Patel, R., Lai, B., Vogt, S., and Fahrni, C. J. (2005) Imaging of the Intracellular Topography of Copper with a Fluorescent Sensor and by Synchrotron X-Ray Fluorescence Microscopy. *Proc. Natl. Acad. Sci. U. S. A. 102*, 11179−11184.
(61) Lim, C. S., Han, J. H., Kim, C. W., Kang, M. Y., Kang, D. W., and Cho, B. R. (2011) A Copper(I)-Ion Selective Two-Photon Fluorescent Probe for in Vivo Imaging. *Chem. Commun. 47*, 7146−7148.
(62) Morgan, M. T., Bagchi, P., and Fahrni, C. J. (2011) Designed to Dissolve: Suppression of Colloidal Aggregation of Cu(I)-Selective Fluorescent Probes in Aqueous Buffer and in-Gel Detection of a Metallochaperone. *J. Am. Chem. Soc. 133*, 15906−15909.
(63) Zeng, L., Miller, E. W., Pralle, A., Isacoff, E. Y., and Chang, C. J. (2006) A Selective Turn-on Fluorescent Sensor for Imaging Copper in Living Cells. *J. Am. Chem. Soc. 128*, 10−11.
(64) Domaille, D. W., Zeng, L., and Chang, C. J. (2010) Visualizing Ascorbate-Triggered Release of Labile Copper within Living Cells using a Ratiometric Fluorescent Sensor. *J. Am. Chem. Soc. 132*, 1194−1195.
(65) Dodani, S. C., Leary, S. C., Cobine, P. A., Winge, D. R., and Chang, C. J. (2011) A Targetable Fluorescent Sensor Reveals that Copper-Deficient SCO1 and SCO2 Patient Cells Prioritize Mitochondrial Copper Homeostasis. *J. Am. Chem. Soc. 133*, 8606−8616.
(66) Godwin, H., and Berg, J. (1996) A Fluorescent Zinc Probe Based on Metal-Induced Peptide Folding. *J. Am. Chem. Soc. 118*, 6514−6515.
(67) Torrado, A., and Imperiali, B. (1996) New Synthetic Amino Acids for the Design and Synthesis of Peptide-Based Metal Ion Sensors. *J. Org. Chem. 61*, 8940−8948.
(68) Walkup, G., and Imperiali, B. (1997) Fluorescent Chemosensors for Divalent Zinc Based on Zinc Finger Domains. Enhanced Oxidative Stability, Metal Binding Affinity, and Structural and Functional Characterization. *J. Am. Chem. Soc. 119*, 3443−3450.
(69) Pearce, D., Walkup, G., and Imperiali, B. (1998) Peptidyl Chemosensors Incorporating a FRET Mechanism for Detection of Ni(II). *Bioorg. Med. Chem. Lett. 8*, 1963−1968.
(70) Deo, S., and Godwin, H. (2000) A Selective, Ratiometric Fluorescent Sensor for Pb^2. *J. Am. Chem. Soc. 122*, 174−175.
(71) Pearce, D., Jotterand, N., Carrico, I., and Imperiali, B. (2001) Derivatives of 8-Hydroxy-2-Methylquinoline are Powerful Prototypes for Zinc Sensors in Biological Systems. *J. Am. Chem. Soc. 123*, 5160−5161.
(72) Shults, M., Pearce, D., and Imperiali, B. (2003) Modular and Tunable Chemosensor Scaffold for Divalent Zinc. *J. Am. Chem. Soc. 125*, 10591−10597.
(73) Walkup, G., and Imperiali, B. (1998) Stereoselective Synthesis of Fluorescent Alpha-Amino Acids Containing Oxine (8-Hydroxyquinoline) and their Peptide Incorporation in Chemosensors for Divalent Zinc. *J. Org. Chem. 63*, 6727−6731.
(74) Mank, M., and Griesbeck, O. (2008) Genetically Encoded Calcium Indicators. *Chem. Rev. 108*, 1550−1564.
(75) Vinkenborg, J. L., Koay, M. S., and Merkx, M. (2010) Fluorescent Imaging of Transition Metal Homeostasis using Genetically Encoded Sensors. *Curr. Opin. Chem. Biol. 14*, 231−237.
(76) Baird, G., Zacharias, D., and Tsien, R. (1999) Circular Permutation and Receptor Insertion within Green Fluorescent Proteins. *Proc. Natl. Acad. Sci. U. S. A. 96*, 11241−11246.
(77) Nagai, T., Sawano, A., Park, E., and Miyawaki, A. (2001) Circularly Permuted Green Fluorescent Proteins Engineered to Sense Ca2. *Proc. Natl. Acad. Sci. U. S. A. 98*, 3197−3202.
(78) Zhao, Y., Araki, S., Jiahui, W., Teramoto, T., Chang, Y., Nakano, M., Abdelfattah, A. S., Fujiwara, M., Ishihara, T., Nagai, T., and Campbell, R. E. (2011) An Expanded Palette of Genetically Encoded Ca^{2+} Indicators. *Science 333*, 1888−1891.
(79) Lindenburg, L., and Merkx, M. (2012) Colorful Calcium Sensors. *ChemBioChem. 13*, 349−351.
(80) Mizuno, T., Murao, K., Tanabe, Y., Oda, M., and Tanaka, T. (2007) Metal-Ion-Dependent GFP Emission in Vivo by Combining a Circularly Permutated Green Fluorescent Protein with an Engineered Metal-Ion-Binding Coiled-Coil. *J. Am. Chem. Soc. 129*, 11378−11383.
(81) Miyawaki, A., Llopis, J., Heim, R., McCaffery, J. M., Adams, J. A., Ikura, M., and Tsien, R. Y. (1997) Fluorescent Indicators for Ca^{2+}-Based on Green Fluorescent Proteins and Calmodulin. *Nature 388*, 882−887.
(82) Miyawaki, A., Griesbeck, O., Heim, R., and Tsien, R. Y. (1999) Dynamic and Quantitative Ca^{2+} Measurements using Improved Cameleons. *Proc. Natl. Acad. Sci. U. S. A. 96*, 2135−2140.
(83) Griesbeck, O., Baird, G. S., Campbell, R. E., Zacharias, D. A., and Tsien, R. Y. (2001) Reducing the Environmental Sensitivity of Yellow Fluorescent Protein. *J. Biol. Chem. 276*, 29188−29194.
(84) Ishii, K., Hirose, K., and Iino, M. (2006) Ca^{2+} Shuttling between Endoplasmic Reticulum and Mitochondria Underlying Ca^{2+} Oscillations. *EMBO Rep. 7*, 390−396.
(85) Palmer, A. E., Giacomello, M., Kortemme, T., Hires, S. A., Lev-Ram, V., Baker, D., and Tsien, R. Y. (2006) Ca^{2+} Indicators Based on Computationally Redesigned Calmodulin-Peptide Pairs. *Chem. Biol. 13*, 521−530.
(86) Palmer, A. E., Jin, C., Reed, J. C., and Tsien, R. Y. (2004) Bcl-2-Mediated Alterations in Endoplasmic Reticulum Ca^{2+} Analyzed with an Improved Genetically Encoded Fluorescent Sensor. *Proc. Natl. Acad. Sci. U. S. A. 101*, 17404−17409.
(87) McCombs, J. E., Gibson, E. A., and Palmer, A. E. (2010) Using a Genetically Targeted Sensor to Investigate the Role of Presenilin-1 in ER Ca^{2+} Levels and Dynamics. *Molecular BioSystems 6*, 1640−1649.
(88) Wallace, D. J., zum Alten Borgloh, S. M., Astori, S., Yang, Y., Bausen, M., Kugler, S., Palmer, A. E., Tsien, R. Y., Sprengel, R., Kerr, J. N. D., Denk, W., and Hasan, M. T. (2008) Single-Spike Detection in Vitro and in Vivo with a Genetic Ca^{2+} Sensor. *Nature Methods. 5*, 797−804.
(89) Heim, N., and Griesbeck, O. (2004) Genetically Encoded Indicators of Cellular Calcium Dynamics Based on Troponin C and Green Fluorescent Protein. *J. Biol. Chem. 279*, 14280−14286.
(90) Mank, M., Reiff, D. F., Heim, N., Friedrich, M. W., Borst, A., and Griesbeck, O. (2006) A FRET-Based Calcium Biosensor with Fast Signal Kinetics and High Fluorescence Change. *Biophys. J. 90*, 1790−1796.
(91) Heim, N., Garaschuk, O., Friedrich, M. W., Mank, M., Milos, R. I., Kovalchuk, Y., Konnerth, A., and Griesbeck, O. (2007) Improved Calcium Imaging in Transgenic Mice Expressing a Troponin C-Based Biosensor. *Nature Methods 4*, 127−129.
(92) Mank, M., Santos, A. F., Direnberger, S., Mrsic-Flogel, T. D., Hofer, S. B., Stein, V., Hendel, T., Reiff, D. F., Levelt, C., Borst, A., Bonhoeffer, T., Hubener, M., and Griesbeck, O. (2008) A Genetically Encoded Calcium Indicator for Chronic in Vivo Two-Photon Imaging. *Nature Methods 5*, 805−811.
(93) van Dongen, E. M. W. M., Dekkers, L. M., Spijker, K., Meijer, E. W., Klomp, L. W. J., and Merkx, M. (2006) Ratiometric Fluorescent Sensor Proteins with Subnanomolar Affinity for Zn(II) Based on Copper Chaperone Domains. *J. Am. Chem. Soc. 128*, 10754−10762.
(94) van Dongen, E. M. W. M., Evers, T. H., Dekkers, L. M., Meijer, E. W., Klomp, L. W. J., and Merkx, M. (2007) Variation of Linker Length in Ratiometric Fluorescent Sensor Proteins Allows Rational

Tuning of Zn(II) Affinity in the Picomolar to Femtomolar Range. *J. Am. Chem. Soc. 129*, 3494−3495.
(95) Vinkenborg, J. L., Nicolson, T. J., Bellomo, E. A., Koay, M. S., Rutter, G. A., and Merkx, M. (2009) Genetically Encoded FRET Sensors to Monitor Intracellular Zn^{2+} Homeostasis. *Nature Methods 6*, 737−740.
(96) Evers, T. H., Appelhof, M. A. M., Meijer, E. W., and Merkx, M. (2008) His-Tags as Zn(II) Binding Motifs in a Protein-Based Fluorescent Sensor. *Protein Eng. Des. Sel. 21*, 529−536.
(97) Evers, T. H., Appelhof, M. A. M., de Graaf-Heuvelmans, P. T. H. M., Meijer, E. W., and Merkx, M. (2007) Ratiometric Detection of Zn(II) using Chelating Fluorescent Protein Chimeras. *J. Mol. Biol. 374*, 411−425.
(98) Dittmer, P. J., Miranda, J. G., Gorski, J. A., and Palmer, A. E. (2009) Genetically Encoded Sensors to Elucidate Spatial Distribution of Cellular Zinc. *J. Biol. Chem. 284*, 16289−16297.
(99) Qiao, W., Mooney, M., Bird, A. J., Winge, D. R., and Eide, D. J. (2006) Zinc Binding to a Regulatory Zinc-Sensing Domain Monitored in Vivo by using FRET. *Proc. Natl. Acad. Sci. U. S. A. 103*, 8674−8679.
(100) Bird, A. J., McCall, K., Kramer, M., Blankman, E., Winge, D. R., and Eide, D. J. (2003) Zinc Fingers can Act as Zn^{2+} Sensors to Regulate Transcriptional Activation Domain Function. *EMBO J. 22*, 5137−5146.
(101) Wang, Z., Feng, L. S., Matskevich, V., Venkataraman, K., Parasuram, P., and Laity, J. H. (2006) Solution Structure of a Zap1 Zinc-Responsive Domain Provides Insights into Metalloregulatory Transcriptional Repression in Saccharomyces Cerevisiae. *J. Mol. Biol. 357*, 1167−1183.
(102) Qin, Y., Dittmer, P. J., Park, J. G., Jansen, K. B., and Palmer, A. E. (2011) Measuring Steady-State and Dynamic Endoplasmic Reticulum and Golgi Zn^{2+} with Genetically Encoded Sensors. *Proc. Natl. Acad. Sci. U. S. A. 108*, 7351−7356.
(103) Gralla, E. B., Thiele, D. J., Silar, P., and Valentine, J. S. (1991) ACE1, a Copper-Dependent Transcription Factor, Activates Expression of the Yeast Copper, Zinc Superoxide Dismutase Gene. *Proc. Natl. Acad. Sci. U. S. A. 88*, 8558−8562.
(104) Thorvaldsen, J. L., Sewell, A. K., McCowen, C. L., and Winge, D. R. (1993) Regulation of Metallothionein Genes by the ACE1 and AMT1 Transcription Factors. *J. Biol. Chem. 268*, 12512−8.
(105) Wegner, S. V., Arslan, H., Sunbul, M., Yin, J., and He, C. (2010) Dynamic Copper(I) Imaging in Mammalian Cells with a Genetically Encoded Fluorescent Copper(I) Sensor. *J. Am. Chem. Soc. 132*, 2567−2569.
(106) Pufahl, R., Singer, C., Peariso, K., Lin, S., Schmidt, P., Fahrni, C., Culotta, V., PennerHahn, J., and OHalloran, T. (1997) Metal Ion Chaperone Function of the Soluble Cu(I) Receptor Atx1. *Science 278*, 853−856.
(107) Rae, T., Schmidt, P., Pufahl, R., Culotta, V., and O'Halloran, T. (1999) Undetectable Intracellular Free Copper: The Requirement of a Copper Chaperone for Superoxide Dismutase. *Science 284*, 805−808.
(108) Joshi, A., Serpe, M., and Kosman, D. J. (1999) Evidence for (Mac1p)2·DNA Ternary Complex Formation in Mac1p-Dependent Transactivation at the CTR1 Promoter. *J. Biol. Chem. 274*, 218−226.
(109) Wegner, S. V., Sun, F., Hernandez, N., and He, C. (2011) The Tightly Regulated Copper Window in Yeast. *Chem. Commun. 47*, 2571−2573.
(110) Tsien, R. Y., and Zucker, R. S. (1986) Control of Cytoplasmic Calcium with Photolabile Tetracarboxylate 2-Nitrobenzhydrol Chelators. *Biophys. J. 50*, 843−853.
(111) Kaplan, J. H., and Ellis-Davies, G. C. R. (1988) Photolabile Chelators for the Rapid Photorelease of Divalent Cations. *Proc. Natl. Acad. Sci. U. S. A. 85*, 6571−6575.
(112) Ellis-Davies, G. C. R., and Kaplan, J. H. (1988) A New Class of Photolabile Chelators for the Rapid Release of Divalent-Cations - Generation of Caged-Ca and Caged-mg. *J. Org. Chem. 53*, 1966−1969.
(113) Wadel, K., Neher, E., and Sakaba, T. (2007) The Coupling between Synaptic Vesicles and Ca^{2+} Channels Determines Fast Neurotransmitter Release. *Neuron 53*, 563−575.
(114) Lou, X., Scheuss, V., and Schneggenburger, R. (2005) Allosteric Modulation of the Presynaptic Ca^{2+} Sensor for Vesicle Fusion. *Nature 435*, 497−501.
(115) Yao, L., and Sakaba, T. (2010) CAMP Modulates Intracellular Ca^{2+} Sensitivity of Fast-Releasing Synaptic Vesicles at the Calyx of Held Synapse. *J. Neurophysiol. 104*, 3250−3260.
(116) Takeshi, S. (2008) Two Ca^{2+}-Dependent Steps Controlling Synaptic Vesicle Fusion and Replenishment at the Cerebellar Basket Cell Terminal. *Neuron 57*, 406−419.
(117) Hosoi, N., Sakaba, T., and Neher, E. (2007) Quantitative Analysis of Calcium-Dependent Vesicle Recruitment and its Functional Role at the Calyx of Held Synapse. *J. Neurosci. 27*, 14286−14298.
(118) Egger, M., Porzig, H., Niggli, E., and Schwaller, B. (2005) Rapid Turnover of the "functional" Na^{+}−Ca^{2+} Exchanger in Cardiac Myocytes Revealed by an Antisense Oligodeoxynucleotide Approach. *Cell Calcium 37*, 233−243.
(119) Mulligan, S. J., and MacVicar, B. A. (2004) Calcium Transients in Astrocyte Endfeet Cause Cerebrovascular Constrictions. *Nature 431*, 195−199.
(120) Takano, T., Tian, G., Peng, W., Lou, N., Libionka, W., Han, X., and Nedergaard, M. (2006) Astrocyte-Mediated Control of Cerebral Blood Flow. *Nature Neurosci. 9*, 260−267.
(121) Hosoi, N., Holt, M., and Sakaba, T. (2009) Calcium Dependence of Exo- and Endocytotic Coupling at a Glutamatergic Synapse. *Neuron 63*, 216−229.
(122) Lu, X., Ellis-Davies, G. C. R., and Levitan, E. S. (2003) Calcium Requirements for Exocytosis do Not Delimit the Releasable Neuropeptide Pool. *Cell Calcium 33*, 267−271.
(123) Millar, A. G., Zucker, R. S., Ellis-Davies, G. C. R., Charlton, M. P., and Atwood, H. L. (2005) Calcium Sensitivity of Neurotransmitter Release Differs at Phasic and Tonic Synapses. *J. Neurosci. 25*, 3113−3125.
(124) Parpura, V., and Haydon, P. G. (2000) Physiological Astrocytic Calcium Levels Stimulate Glutamate Release to Modulate Adjacent Neurons. *Proc. Natl. Acad. Sci. U. S. A. 97*, 8629−8634.
(125) Pawlicki, M., Collins, H. A., Denning, R. G., and Anderson, H. L. (2009) Two-Photon Absorption and the Design of Two-Photon Dyes. *Angew. Chem. -Int. Edit. 48*, 3244−3266.
(126) Ellis-Davies, G. C. R. (2011) Two-Photon Microscopy for Chemical Neuroscience. *ACS Chem. Neurosci. 2*, 185−197.
(127) Brown, E., Shear, J., Adams, S., Tsien, R., and Webb, W. (1999) Photolysis of Caged Calcium in Femtoliter Volumes using Two-Photon Excitation. *Biophys. J. 76*, 489−499.
(128) Helmchen, F., and Denk, W. (2005) Deep Tissue Two-Photon Microscopy. *Nat. Methods 2*, 932−940.
(129) Momotake, A., Lindegger, N., Niggli, E., Barsotti, R., and Ellis-Davies, G. (2006) The Nitrodibenzofuran Chromophore: A New Caging Group for Ultra-Efficient Photolysis in Living Cells. *Nature Methods 3*, 35−40.
(130) Sutherland, D. E. K., and Stillman, M. J. (2011) The ″Magic Numbers" of Metallothionein. *Metallomics. 3*, 444−463.
(131) Gwizdala, C., Kennedy, D. P., and Burdette, S. C. (2009) ZinCast-1: A Photochemically Active Chelator for Zn^{2}. *Chem. Commun.*, 6967−6969.
(132) Mbatia, H. W., Kennedy, D. P., Camire, C. E., Incarvito, C. D., and Burdette, S. C. (2010) Buffering Heavy Metal Ions with Photoactive CrownCast Cages. *Eur. J. Inorg. Chem. 2010*, 5069−5078.
(133) Kennedy, D. P., Gwizdala, C., and Burdette, S. C. (2009) Methods for Preparing Metal Ion Photocages: Application to the Synthesis of CrownCast. *Org. Lett. 11*, 2587−2590.
(134) Kennedy, D. P., Incarvito, C. D., and Burdette, S. C. (2010) FerriCast: A Macrocyclic Photocage for Fe^{3}. *Inorg. Chem. 49*, 916−923.
(135) Bandara, H. M., Kennedy, D. P., Akin, E., Incarvito, C. D., and Burdette, S. C. (2009) Photoinduced Release of Zn^{2+} with ZinCleav-1: A Nitrobenzyl-Based Caged Complex. *Inorg. Chem. 48*, 8445−8455.
(136) Bandara, H. M. D., Walsh, T. P., and Burdette, S. C. (2011) A Second-Generation Photocage for Zn^{2+} Inspired by TPEN: Character-

ization and Insight into the Uncaging Quantum Yields of ZinCleav Chelators. *Chem.—Eur. J. 17*, 3932−3941.
(137) Mbatia, H. W., Bandara, H. M. D., and Burdette, S. C. (2012) CuproCleav-1, a First Generation Photocage for Cu. *Chem. Commun. 48*, 5331−5333.
(138) Ciesienski, K. L., Haas, K. L., Dickens, M. G., Tesema, Y. T., and Franz, K. J. (2008) A Photolabile Ligand for Light-Activated Release of Caged Copper. *J. Am. Chem. Soc. 130*, 12246−12247.
(139) Ciesienski, K. L., Hyman, L. M., Yang, D. T., Haas, K. L., Dickens, M. G., Holbrook, R. J., and Franz, K. J. (2010) A Photo-Caged Platinum(II) Complex that Increases Cytotoxicity upon Light Activation. *Eur. J. Inorg. Chem. 2010*, 2224−2228.
(140) Ciesienski, K. L., Haas, K. L., and Franz, K. J. (2010) Development of Next-Generation Photolabile Copper Cages with Improved Copper Binding Properties. *Dalton Trans.*, 9538−9546.
(141) Dodani, S. C., He, Q., and Chang, C. J. (2009) A Turn-on Fluorescent Sensor for Detecting Nickel in Living Cells. *J. Am. Chem. Soc. 131*, 18020−18021.
(142) Wegner, S. V., Ertem, E., Sunbul, M., and He, C. (2011) Metal-Binding Properties of Hpn from Helicobacter Pylori and Implications for the Therapeutic Activity of Bismuth. *Chem. Sci. 2*, 451−456.